Polymer Chemistry

Accepted Manuscript

This is an *Accepted Manuscript*, which has been through the Royal Society of Chemistry peer review process and has been accepted for publication.

Accepted Manuscripts are published online shortly after acceptance, before technical editing, formatting and proof reading. Using this free service, authors can make their results available to the community, in citable form, before we publish the edited article. We will replace this *Accepted Manuscript* with the edited and formatted *Advance Article* as soon as it is available.

You can find more information about *Accepted Manuscripts* in the Information for Authors.

Please note that technical editing may introduce minor changes to the text and/or graphics, which may alter content. The journal's standard Terms & Conditions and the Ethical guidelines still apply. In no event shall the Royal Society of Chemistry be held responsible for any errors or omissions in this *Accepted Manuscript* or any consequences arising from the use of any information it contains.

ROYAL SOCIETY OF CHEMISTRY

www.rsc.org/polymers

Fluorinated Bottlebrush Polymers Based on Poly(trifluoroethyl methacrylate): Synthesis and Characterizations

Yuewen Xu,[*a] Weiyu Wang,[b] Yangyang Wang,[a] Jiahua Zhu,[a] David Uhrig,[a] Xinyi Lu,[b] Jong K. Keum,[a] Jimmy W. Mays,[b] Kunlun Hong[*a]

[a] Center for Nanophase Materials Sciences, Oak Ridge National Laboratory, Oak Ridge, TN 37831, USA

[b] Department of Chemistry, University of Tennessee, Knoxville, TN 37996, USA

Abstract

Bottlebrush polymers are densely grafted polymers with long side-chains attached to a linear polymeric backbone. Their unusual structures endow them with a number of unique and potentially useful properties in solution, in thin films, and in bulk. Despite the many studies of bottlebrushes reported, the structure-property relationships for this class of materials are still poorly understood. In this contribution, we report the synthesis and characterizations of fluorinated bottlebrush polymers based on poly(2,2,2-trifluoroethyl methacrylate). The synthesis was achieved by atom transfer radical polymerization (ATRP) using an α-bromoisobutyryl bromide functionalized norbornene initiator, followed by ring-opening metathesis polymerization (ROMP) using the third generation Grubbs' catalyst (**G3**). Rheological characterization revealed that the bottlebrush polymer backbones remained unentangled as indicated by the lack of a rubbery plateau in modulus. By tuning the size of the backbone of the bottlebrush polymers, near-spherical and elongated particles representing single brush molecular morphologies were observed in a good solvent as evidenced by TEM imaging, suggesting a semi-flexible nature of their backbones in dilute solutions. Thin films of bottlebrush polymers exhibited noticeably

higher static water contact angles as compared to that of the macromonomer reaching the hydrophobic regime, where little differences were observed between each bottlebrush polymer. Further investigation by AFM revealed that the surface of the macromonomer film was relatively smooth; in contrast, the surface of bottlebrush polymers displayed certain degrees of nano-scale roughness (R_q = 0.8–2.4 nm). The enhanced hydrophobicity of these bottlebrushes is likely resulted from the preferential enrichment of the fluorine containing end groups at the periphery of the molecules and film surface due to the side chain crowding effect. Our results provide key information towards design of architecturally tailored fluorinated polymers with desirable properties.

Introduction

Bottlebrush polymers or molecular brushes are macromolecules with densely grafted polymeric side-chains. They represent are a unique class of materials inspired by brush-like proteoglycans.[1,2] Their morphological and physical properties are dictated by the grafting density and side chain length.[3] The unique structures of bottlebrush polymers allow them to find potential applications in a variety of fields, including drug delivery in biological system,[4,5] smart responsive materials,[6,7] photonic crystals when large domain bottlebrush block copolymers are achieved.[8,9] While some distinctive properties of bottlebrush polymers in relation to molecular conformation have been disclosed, little is known about the surface properties of bottlebrush films.

Fluorinated polymers are among the most important coating materials because of their low surface energy, chemical resistance, and low refractive index.[10-16] 2,2,2-Trifluororoethyl methacrylate (TFEMA), representing a class of lightly fluorinated monomer, exhibits hybrid properties of acrylics and fluoro-polymers upon either homo-polymerization or copolymerization with other acrylic monomers.[17] These polymers could be further developed into coating and adhesive materials.[18,19] On the other hand, the synthesis of poly(trifluoroethyl methacrylate) (PTFEMA) in a controlled manner has

been challenging. Hu and co-workers investigated the atom transfer radical polymerization (ATRP) of this monomer with various ligands, and modestly controlled polymerization with regarding to molar mass and polydispersity was achieved when 2,2'-bipyridine was used as ligand.[20] Narita et al. reported anionic polymerization of such monomers using different organolithium or organomagnesium initiators with relatively low polydispersities and appreciable yields in THF and toluene.[21] Triblock copolymers based on poly(methacrylic acid), poly(benzyl methacrylate) (PBzMA), and PTFEMA were also prepared by reversible addition–fragmentation chain transfer polymerization (RAFT).[22] Microphase separation between the mutually incompatible PBzMA and semi-fluorinated PTFEMA blocks produced a range of complex morphologies in solutions. However, little progress has been made to obtain end-functionalized PTFEMA, which is essential to construct well-defined complex architectures, including bottlebrush polymers. Furthermore, the impact of PTFEMA polymer architecture on material properties is largely unexplored. We sought to take advantage of the versatility of ATRP to synthesize norbornene end-functionalized PTFEMA that could be further used as macromonomers for the synthesis of bottlebrush polymers, and thus many basic properties of the bottlebrushes can be assessed.

The aim of this work is to generate well-defined bottlebrush polymers with PTFEMA side chains and polynorbornene backbone, and to understand the impact of molecular architecture and fluorination on the fundamental material properties. By employing ring-opening metathesis polymerization (ROMP) of norbornene end-functionalized PTFEMA, bottlebrush polymers with well-controlled structures, molar masses and grafting densities have been prepared. In contrast to other synthetic approaches to bottlebrush polymers (i.e., graft from and graft onto), this "grafting through" route renders exceptional control of side chain grafting densities along the backbone, meaning that the PTFEMA side chains are guaranteed to distribute regularly along each repeating unit of polynorbornene backbones.[23,24] The unique molecular architecture of

polynorbornene-*graft*-poly (trifluoroethyl methacrylate) (PNB-*g*-PTFEMA) bottlebrush polymers may lead to certain intriguing properties that cannot otherwise be found in their homopolymers or simple block copolymers. Their bulk properties, i.e., rheological and thermal properties, their self-assembled morphologies in solution, and surface properties of these thin films are investigated.

Results and discussion

Synthesis of Bottlebrush Polymers. The synthetic route towards fluorinated bottlebrushes is shown in Scheme 1. In the first step, the α-bromoisobutyryl bromide functionalized norbornene (Br-NB **2**) was prepared by a reported procedure and was utilized as the ATRP initiator.[25] Copper (I) chloride was used as the catalyst in this case due to the slower polymerization rate as compared to copper (I) bromide, which is important in maintaining a relatively low macromonomer molecular weight.[26] Generally, a high molar mass macromonomer is undesirable in the synthesis of bottlebrushes because of steric effects leading to low conversions.[27] When copper (I) bromide was used in a control experiment, the molar mass of the resulting macromonomer was much higher than that obtained from copper (I) chloride under the similar polymerization conditions (11 kg mol^{-1} vs. 3.5 kg mol^{-1}, see Table 1). As a result, the macromonomer conversion in the ROMP was as low as 55% for macromonomer $PTFEMA_{66}$ (Table 1). In contrast, the shorter macromonomer, $PTFEMA_{22}$, gives significantly higher conversions and higher degrees of polymerization for bottlebrush backbones (DP up to 200, Table 1).

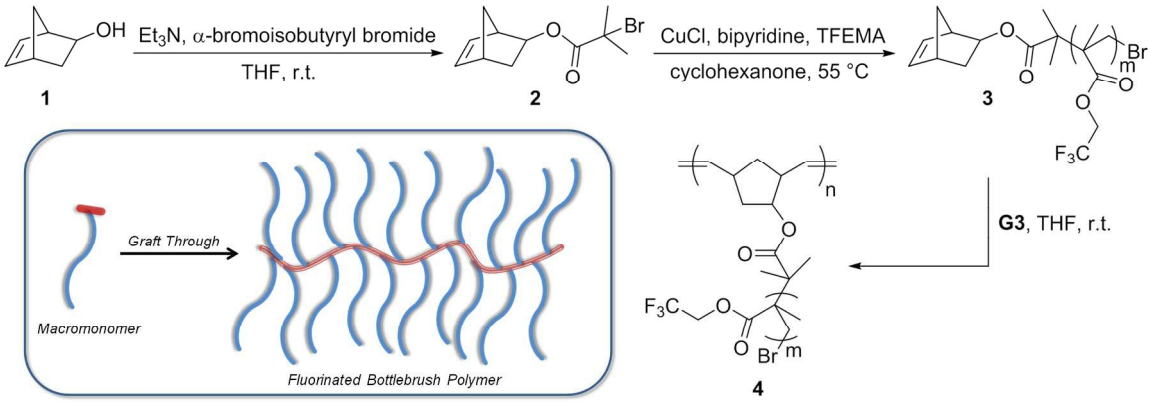

Scheme 1. Synthetic Scheme of Poly(trifluoroethyl methacrylate) Bottlebrush Polymer. Inset: cartoon of ROMP of macromonomer yielding bottlebrush polymer through a "graft-through" manner. Note: for ATRP of a high molar mass macromonomer, $PTFEMA_{66}$, the polymerization was carried out at 70 °C (30 min) and CuBr was used as the catalyst.

Table 1. Molecular Characteristics of Polymers

Entry	[M]/[G3][a]	M_n, kg mol^{-1} (Calculated)	M_n, kg mol^{-1} (LS-SEC)[b]	$Đ$	Conv.[d] (%)	T_g
$PTFEMA_{66}$	NA		11.0[c]	1.26		59
PNB_{49}-*g*-$PTFEMA_{66}$	40	440	510	1.10	55	70
$PTFEMA_{22}$	NA		3.5[c]	1.09		55
PNB_{21}-*g*-$PTFEMA_{22}$	15	56	79	1.05	98	64
PNB_{49}-*g*-$PTFEMA_{22}$	40	150	180	1.07	> 99	65
PNB_{200}-*g*-$PTFEMA_{22}$[e]	150	560	760	1.10	97[f]	68[g]

[a] Monomer to catalyst loading ratio; [b] the *dn/dc* of macromonomer and bottlebrush is 0.0372 mL/g in EtOAc; [c] determined from NMR end group analysis; [d] compared by monomer and bottlebrush peak areas from SEC-RI signals; [e] the first number on bottlebrush polymer (21, 49, and 200) corresponds to the number of repeating unit on backbone; the second number (22) indicates the number of repeating unit on side chain. There will be grafted side chains on every norbornene repeating unit; [f] after dialysis to

remove unreacted macromonomers; conversion of 88% prior to dialysis; [g] the glass transition temperature of pure polynorbornene prepared from ROMP is ~ 31 °C.[28]

The structural characterization of the polymers was first conducted using proton NMR, as illustrated in Figure 1a. The resonances at 6.32–5.98 ppm of macromonomer **3** correspond to the vinyl peaks of norbornene functionality (Figure 1a top), indicating an efficient initiation of trifluoroethyl methacrylate monomer with the α-bromoisobutyryl bromide initiator from ATRP.[25] The formed PTFEMA macromonomers were further polymerized by ROMP with the highly efficient **G3** catalyst to give the bottlebrush polymer. The vinyl resonance of norbornene disappeared and was replaced with two broad peaks at 5.32 and 4.97 ppm, which were assigned to the vinyl resonances on the polynorbornene backbone, indicating a successful polymerization (Figure 1a bottom). The chemical shifts at ~ 4.33 ppm of both macromonomer **3** and bottlebrush **4** were assigned to the protons on $-CH_2CF_3$, and are more downfield than that of a methyl ester group on polymethyl methacrylate (~ 3.7 ppm) due to the strong electron withdrawing ability of the trifluoroethyl group.[20]

The well-defined structure of these bottlebrush polymers was further evidenced by size exclusion chromatography (SEC, Figure 1b). The polydispersity index (***Đ***) remains low (< 1.1) for all three bottlebrush polymers with backbone degrees of polymerization up to 200, showing that a controlled molecular architecture resulted from ROMP. In addition, the polymerization kinetics of ROMP was monitored by molar mass and polydispersity index by taking aliquots at different time. A representative kinetic plot of PNB_{49}-*g*-$PTFEMA_{22}$ is shown in Figure 1c. The number average molecular weight (M_n) remained nearly linear with conversion during the course of the polymerization and the polydispersity was low throughout, both of which support the "living" nature of this ROMP polymerization with **G3** catalyst, despite the steric effects inherent in the macromonomer during the coordination of Ru metal complex to cyclic norbornene end groups.

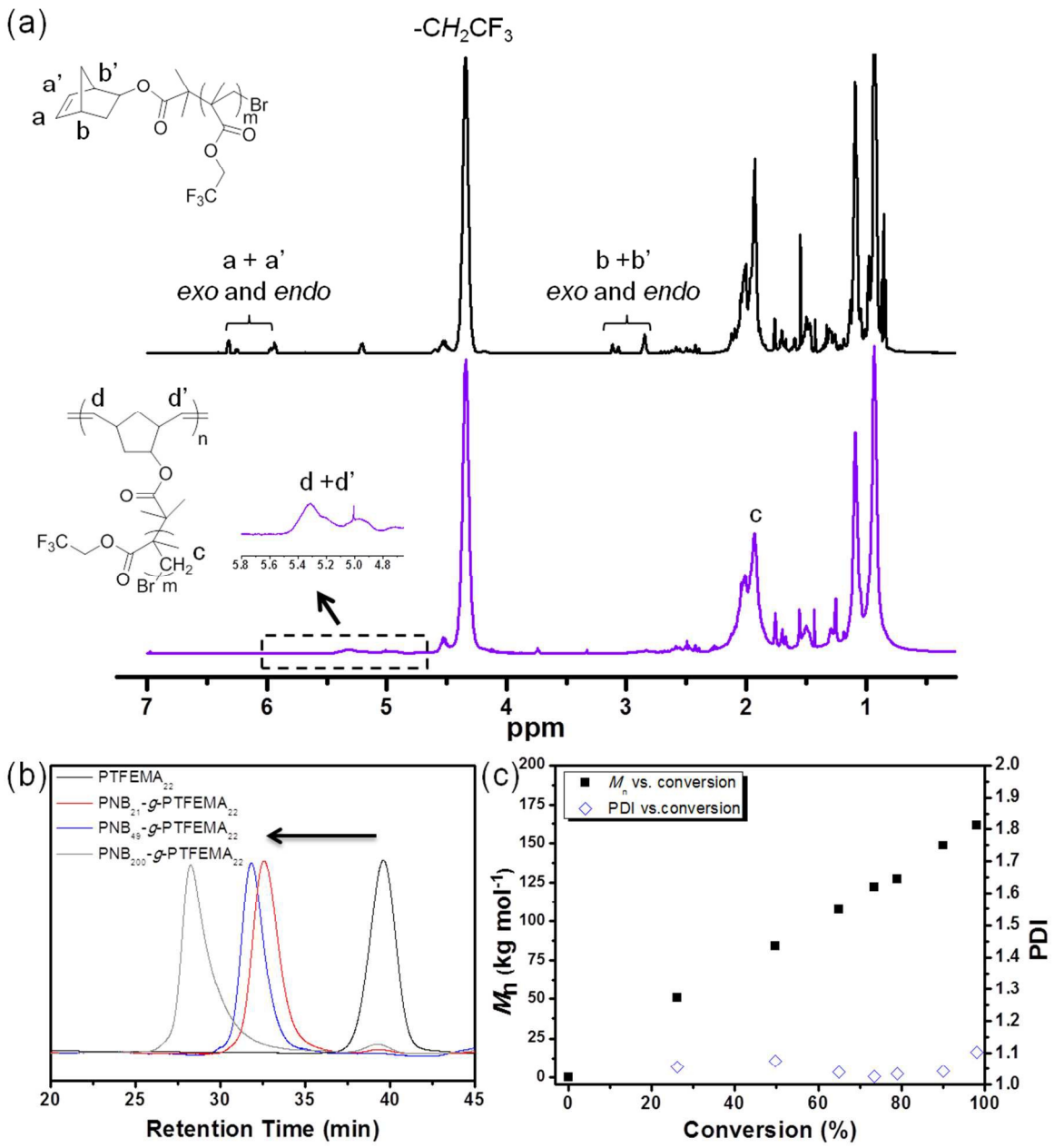

Figure 1. (a) ^{1}H NMR spectra of PTFEMA$_{22}$ macromonomer **3** (top) and PNB$_{49}$-*g*-PTFEMA$_{22}$ bottlebrush polymer **4** (bottom), in $CDCl_3$; (b) SEC traces of macromonomer and bottlebrush polymers; RI detector, ethyl acetate as eluent; (c) representative ROMP kinetics of PNB$_{49}$-*g*-PTFEMA$_{22}$; M_n (solid symbol) and PDI (open symbol) as a function of macromonomer conversion. The polymerization reaches near 100% consumption for backbone length of 21 and 49 within 60 min. The molar mass was determined by light-scattering analysis, whereas the conversion was calculated by the areas of RI signals.

Bulk Material Properties. The bulk properties of bottlebrush polymers are known to be different from its linear counterpart in a variety of aspects, including thermal and rheological properties.[23] Firstly, the glass transition temperatures (T_g) of macromonomer and bottlebrush polymers were measured (Figure 2). The T_g of PTFEMA macromonomer is 55 °C as determined by differential scanning calorimetry (DSC). Upon ROMP of the macromonomer, the T_gs of the resulting bottlebrushes shift slightly to higher temperatures. The T_gs of three bottlebrush polymers exhibit a very weak dependence on the backbone degree of polymerization, as the difference in T_g is marginal (< 4 °C) between PNB_{21}-*g*-$PTFEMA_{22}$ and PNB_{200}-*g*-$PTFEMA_{22}$, although their molar masses are different by nearly an order of magnitude. This result is consistent with the report on polystyrene bottlebrush system by Tsukahara and coworkers.[28] Since the T_g of a polymer is primarily determined by the excess free volume of chain ends per unit, the T_g of bottlebrush polymers should remain constant over a large range of backbone degree of polymerization as long as the side chain length is kept the same.[29-31]

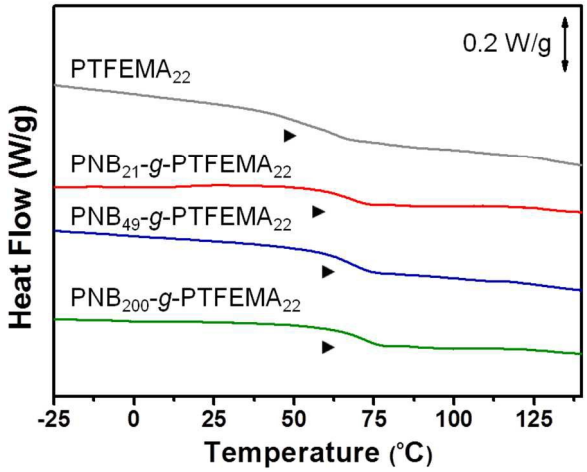

Figure 2. DSC thermograms of macromonomer and bottlebrush polymers with different backbone degree of polymerizations. From 2nd heating curve, 10 °C/min (exothermic up).

The linear viscoelastic (LVE) spectra of PNB_{200}-*g*-$PTFEMA_{22}$ and the macromonomer $PTFEMA_{22}$ are showed in Figure 3(a). Three relaxation processes can be clearly seen in PNB_{200}-*g*-$PTFEMA_{22}$: the segmental relaxation at high frequencies, the grafted chain motion at intermediate frequencies, and the backbone relaxation at low frequencies. From these results, it is clear that the bottlebrushes remain unentangled even

with degree of polymerization of the backbone up to 200, as the characteristic rubbery plateau feature associated with polymer entanglement is absent at low frequencies.[32,33] The temperature shift factors a_T from the Time-Temperature Superposition procedure are shown in Figure 3(b). The a_T of $PTFEMA_{22}$ is distinctly different from those of the bottlebrush polymers, which is consistent with the change of T_g revealed by DSC. On the other hand, while DSC indicates a systematic but subtle variation of T_g among the three bottlebrush polymers, their mechanical temperature shift factors essentially collapse onto a single master curve in the temperature range of our investigation.

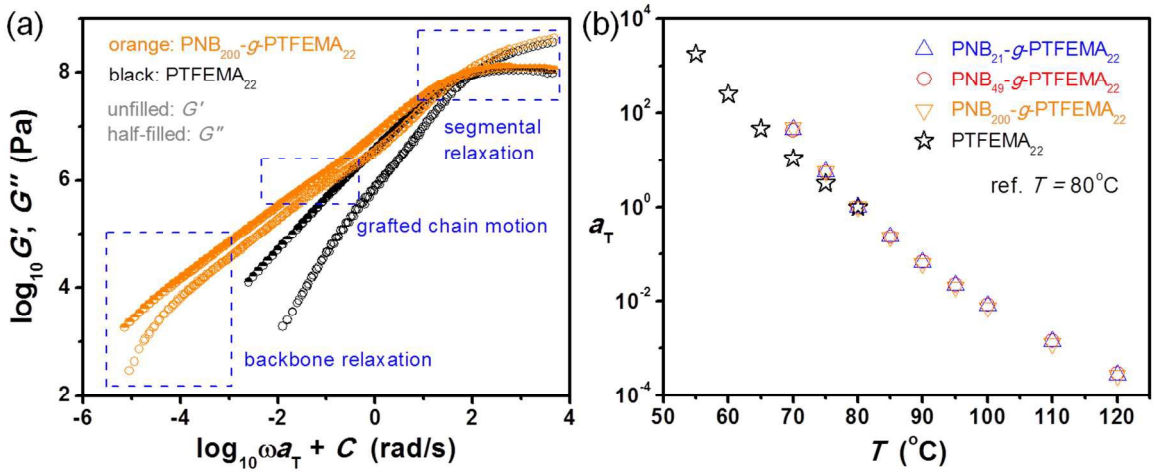

Figure 3. (a) Comparison of the linear viscoelastic spectra of the bottlebrush polymer PNB_{200}-*g*-$PTFEMA_{22}$ and the macromonomer $PTFEMA_{22}$; master curves for all three bottlebrush polymers see supporting information, Figure S6; (b) Temperature shift factor a_T for three bottlebrush polymers and $PTFEMA_{22}$.

Morphologies of Bottlebrushes in Solution. The morphology of a bottlebrush polymer in solution is governed by many factors, mainly the competing force between backbone and side chains.[3] When the backbone length (L) of the bottlebrush is sufficiently shorter than the diameter of side chains (D), it typically shows a spherical or globular morphology in good solvents.[34, 35] In contrast, a cylindrical shape is observed if the aspect ratio is high (L/D > 1).[23] Given that the side chain lengths of these bottlebrush polymers are identical (22 repeating units) and under the assumption that the side chains are fully extended, we would expect the globular to cylindrical shape transition at L/D ~ 1, which corresponds to approximate 20 norbornene repeating units along the backbone for this

PNB-*g*-PTFEMA bottlebrush polymer. Meanwhile, bottlebrush polymers could adopt semi-flexible conformations in a dilute solution, which could be further identified from the TEM images of our bottlebrushes (Figure 4). The bottlebrush polymers were dissolved in a non-selective solvent (EtOAc) at a concentration of 1 mg/mL. Through TEM imaging, we found the PNB_{21}-*g*-$PTFEMA_{22}$ formed isolated near-spherical particles with a diameter of ~ 10 nm in EtOAc solution, corresponding to the morphology of single bottlebrush molecule (Figure 4a). When the L/D ratio increased to 2.5, the bottlebrush polymer adopted an elongated shape (Figure 4b). Upon further increasing the L/D ratio to 10, rather than forming longer cylinders, large "spherical" particles with diameter of ~ 25 nm were observed from TEM (Figure 4c), suggesting the backbone is partially coiling[3] The R_h values for bottlebrush polymers determined from dynamic light scattering (DLS) are 5.8, 6.5, 14.2 nm for PNB_{21}-*g*-$PTFEMA_{22}$, PNB_{49}-*g*-$PTFEMA_{22}$ and PNB_{200}-*g*-$PTFEMA_{22}$, respectively, which correlate decently well with the sizes from TEM. According to our earlier study of polylactic acid (PLA) bottlebrush polymers, an increase in the degree of polymerization of the bottlebrush backbones results in increased persistence length of the flexible cylinder.[36] We expect the flexibility of the backbone chains to decrease as the numbers of norbornene repeat units comprising the backbone are increased for these PNB-*g*-PTFEMA bottlebrush polymers.

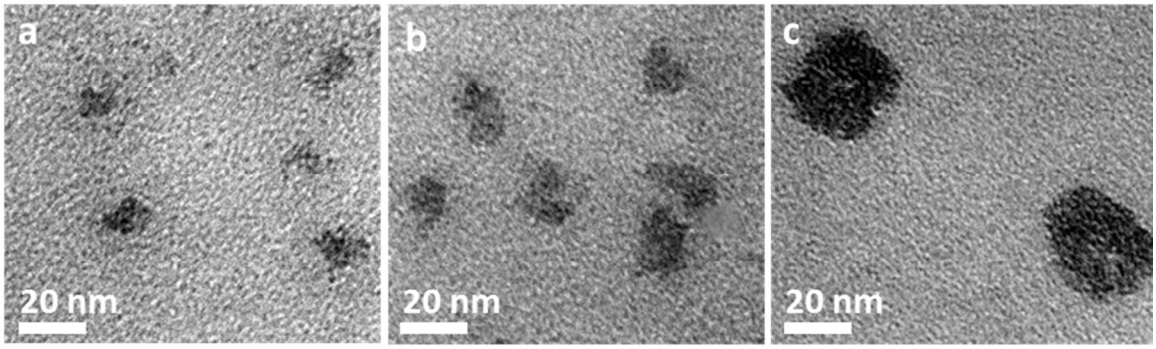

Figure 4. TEM images of bottlebrush: (a) PNB_{21}-*g*-$PTFEMA_{22}$; (b) PNB_{49}-*g*-$PTFEMA_{22}$; (c) PNB_{200}-*g*-$PTFEMA_{22}$. Concentration of 1 mg/mL in EtOAc for all three polymers; scale bars represent 20 nm. The samples were stained with OsO_4 prior to TEM imaging.

Surface Properties. Tremendous efforts have been devoted to the understanding of the influence of structural parameters, such as architectures, end-group functionalities, on the

surface properties of polymeric materials.[37-39] We expected thin films formed from our bottlebrushes to show intriguing surface properties because of the interplay between fluorination and structural constraints. The polymer thin films were prepared by spin coating and the hydrophobicity of these films was tested by static water contact angle measurements. The thin film thickness was kept ~ 400 nm as determined from the SEM cross-section. Furthermore, GI-SAXS data exhibiting an asymptotic decay in scattering with respect to Q implies that there is no large-scale assemblies or ordered structures within the observed length scale (supporting information, Figure S7). Generally, acrylate polymers could be either hydrophilic or hydrophobic depending on their pendant groups. Poly(methyl methacrylate) (PMMA), the most commonly used acrylate polymer, possesses a water contact angle of ~ 68° and is generally considered hydrophilic.[37] The PTFEMA macromonomer is different from PMMA in structure with an extra $–CF_3$ group on each repeating unit and a norbornene chain-end functional group. The low molar mass $PTFEMA_{22}$ macromonomer gives a water contact angle of ~ 80°, driving this acrylate polymer into a more hydrophobic regime as compared to the PMMA, which is consistent with the reported values for PTFEMA with similar molecular weight.[20] Upon polymerization of the TFEMA macromonomer, the water contact angle of the formed bottlebrush polymers displayed a significant shift from hydrophilic into the hydrophobic regime (to > 90°, Table 2 and Figure 5); however, the three bottlebrush polymers with different backbone lengths exhibited negligibly different water contact angles, hence, similar hydrophobicity.

Table 2. Static Water Contact Angle of Polymers

Entry	Water Contact Angle (°)
$PTFEMA_{22}$	79.8 ± 0.5
PNB_{21}-*g*-$TFEMA_{22}$	96.1 ± 0.2
PNB_{49}-*g*-$TFEMA_{22}$	96.7 ± 0.1
PNB_{200}-*g*-$TFEMA_{22}$	96.7 ± 0.1

Note: for $PTFEMA_{66}$ macromonomer, the water contact angle is 85.0 ± 0.2°; the bottlebrush polymer from this macromonomer was not measured due to the low conversion in polymerization (resulted a mixture of macromonomer and bottlebrush).

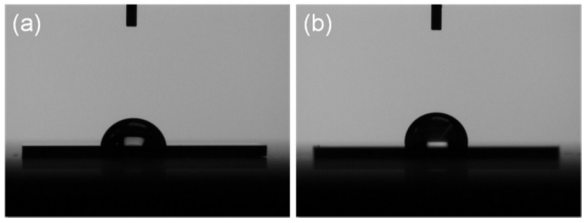

Figure 5. Representative water contact angle images of polymer thin films: (a) macromonomer $PTFEMA_{22}$; (b) bottlebrush polymer (PNB_{49}-*g*-$TFEMA_{22}$). Detailed images for all bottlebrush polymers refer to supporting information (Figure S5).

The difference in surface characteristics between macromonomer and bottlebrush polymers was further probed by atomic force microscopy (AFM). The surface roughness was revealed in the 3D topographical images, as shown in Figure 6, top graphs. The surface of macromonomer thin film is relatively smooth, whereas in contrast, the bottlebrush polymer films exhibit certain degrees of nano-scale roughness, which could be illustrated by the nano-scale cluster segregation or collapse on surface. The calculated rms roughness (R_q) is 0.41, 2.40, 1.21, and 0.80 nm for $PTFEMA_{22}$, PNB_{21}-*g*-$PTFEMA_{22}$, PNB_{49}-*g*-$PTFEMA_{22}$, and PNB_{200}-*g*-$PTFEMA_{22}$, respectively. The height versus surface coordinate profiles of the corresponding cross-sections (Figure 6 top images) are consistent with these rms roughness results (Figure 6 bottom images).

Although the roughness of a polymeric thin film is closely related to its hydrophobicity and a higher degree of roughness usually induces an enhanced hydrophobicity, also known as "lotus effect",[38-42] the difference in contact angle between PTFEMA macromonomer and its bottlebrush polymers may be only partially caused by the surface roughness. More importantly, the side chain morphology along the bottlebrush backbones will likely induce a crowding effect. The configuration of a highly branched polymer could strongly constrain the conformation of side chains.[38] The crowding of PTFEMA branches likely leads to a preferential enrichment of the fluorine

containing end groups at the periphery of the polymers and film surface. As a result, these PNB-based bottlebrush polymers exhibit higher hydrophobicity over the PTFEMA macromonomer itself. Moreover, since the three bottlebrush PNB_{21}-*g*-$PTFEMA_{22}$, PNB_{49}-*g*-$PTFEMA_{22}$, and PNB_{200}-*g*-$PTFEMA_{22}$ possess an identical side chain length, similar density of the CF_3 group should be expected at the periphery of these polymers and film surface. This explains the very subtle changes observed in water contact angles between three bottlebrushes, even though the roughness of their surfaces was noticeably different.

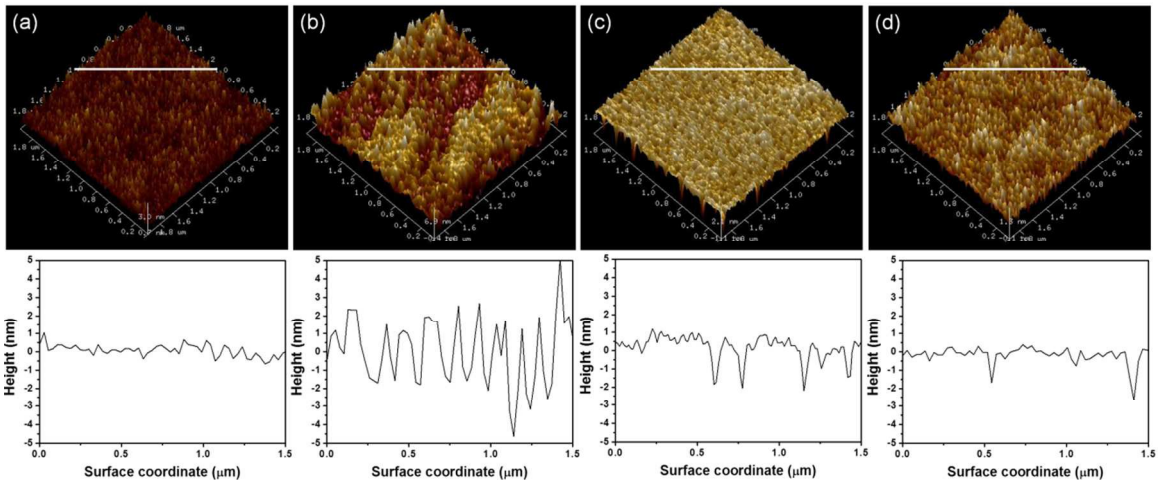

Figure 6. AFM images of (a) macromonomer $PTFEMA_{22}$; (b) bottlebrush PNB_{21}-*g*-$TFEMA_{22}$; (c) bottlebrush PNB_{49}-*g*-$TFEMA_{22}$; (d) bottlebrush PNB_{200}-*g*-$TFEMA_{22}$. Top: 3D topographical images; bottom: representative cross-sections of corresponding 3D images highlighted in white.

Conclusion

To conclude, well-defined bottlebrush polymers with poly(trifluoroethyl methacrylate) (PTFEMA) side chains and polynorbornene backbones were synthesized via sequential ATRP and ROMP polymerizations. Their bulk properties, including rheological and thermal properties, as well as solution morphologies in a good solvent (EtOAc) were evaluated to understand the impact of molecular architectures on material properties. The bottlebrushes displayed distinctively different behaviors from those of macromonomers. The surface behaviors of macromonomers and bottlebrush polymers

were also investigated. The hydrophobicity of these thin films showed a clear difference between macromonomer and bottlebrush polymers, whereas little differences were observed between three bottlebrush polymers. We found that the side chain crowding effect of these bottlebrush polymers played a major role in their surface properties. Our studies on these poly(trifluoroethyl methacrylate) bottlebrush polymers provide technically useful and important information for designing and fabricating fluorinated polymers with desirable functionalities and applications, such as advanced coating materials.

Experimental Section

For detailed materials information, please refer to supporting information.

Synthesis and Methods. *Preparation of poly(2,2,2-trifluoroethyl methacrylate) macromonomer **3**.* The polymerization procedure of 2,2,2-trifluoroethyl methacrylate via atom transfer radical polymerization was modified from a previous report.[20] A Schlenk flask was charged with α-bromoisobutyryl bromide functionalized norbornene (7.72 mmol), 2,2,2-trifluoroethyl methacrylate (154 mmol), dipyridine (23.2 mmol), and cyclohexanone (66 mL). The mixture was degassed by two cycles of freeze-pump-thaw, after which CuCl (7.72 mmol) was introduced into the flask and degassed by another two cycles. The flask was refilled with nitrogen and allowed to react at an elevated temperature. Upon completion (30 min), the reaction mixture was cooled in a liquid nitrogen bath before being exposed to air and precipitated into 1 L hexanes. The solid form collected after filtration was dissolved in 100 mL THF and passed through a neutral Al_2O_3 column to remove the catalyst. The product was isolated by precipitating repeatedly in hexanes. The polymer was dried in vacuum oven overnight to obtain the final product as a white powder. ^{1}H NMR (500 MHz, $CDCl_3$) as *exo* and *endo* isomers; δ 6.32 (m, *endo*), 6.26 (m, *exo*), 5.98-5.94 (m, *exo* and *endo*), 5.20 (m, *endo*), 4.60 (m, *exo*), 4.33 (br, s), 3.12 (s, *endo*), 3.07 (s, *exo*), 2.85 (*exo* and *endo*), 2.68-2.40 (m), 2.01 (m), 1.93 (s), 1.76-1.24 (m), 1.08 (s), 0.93 (s), 0.85 (m). ^{13}C NMR (125 MHz, $CDCl_3$) δ 175.8, 175.5, 174.8, 138.7, 131.6, 126.3, 124.2, 122.0, 119.7, 51.5, 51.2, 47.8, 45.9, 45.2, 45.1, 44.9, 42.4, 41.6, 36.3, 34.9, 34.7, 29.3, 25.5, 19.0, 18.8, 17.0, 11.7. ^{19}F NMR (470 MHz, $CDCl_3$) δ 73.3.

*Preparation of poly(norbornene-g-trifluoroethyl methacrylate) bottlebrush polymer **4** by ROMP.* The macromonomer **3** (0.32 mmol) was dissolved in 52 mL THF and purged with nitrogen for 30 min. The **G3** (0.011 mmol) was dissolved in minimum degassed THF (~ 0.1 mL) and syringed into the flask containing macromonomer. The reaction was allowed to proceed for two hours prior to quenching with 0.8 mL ethyl vinyl ether, and stirred for another 30 min. The polymer was purified by passing it through a short neutral Al_2O_3 column and precipitating it into a copious amount of methanol. The polymer was collected and dried in a vacuum oven overnight to give a white to pale while solid. In the case of kinetic study, aliquot of reaction mixture (0.4 mL) was taken at different time intervals and quenched with ethyl vinyl ether. Each polymer was dried in a vacuum oven before the SEC measurements. ^{1}H NMR (500 MHz, $CDCl_3$) δ 5.32 (s, br), 4.97 (s, br), 4.33 (br, s), 3.74 (m), 3.33 (m), 2.84-2.40 (m), 2.01-1.93 (br, m), 1.76-1.26 (m), 1.09 (br, s), 0.93 (br, s). ^{13}C NMR (125 MHz, $CDCl_3$) δ 175.8, 175.7, 175.4, 174.8, 126.4, 124.2, 121.9, 119.8, 62.7, 62.4, 62.1, 61.4, 61.2, 60.9, 53.5, 45.2, 45.0, 19.3, 18.3, 17.3, 16.5. ^{19}F NMR (470 MHz, $CDCl_3$) δ 73.4.

Dianalysis. Dianalysis was performed with pretreated RC membrane (Spectrum Laboratories) with a molecular weight cut-off of 10 kD. Ethyl acetate was used as solvent, and the total dianalysis time was 20 h.

Preparation of polymer thin films. To prepare the polymer thin films, either macromonomer or bottlebrush was dissolved in EtOAc (20 mg/mL) and filtered through a Millipore membrane (Millex-FG, 0.2 μm). Silicon wafers were cleaned by soaking in deionized water, acetone and isopropanol for one hour in each solvent. Then, polymer solution was spin-cast on the silicon wafer (1500 rpm for 30s and 300 rpm for another 30s). The resulting thin films were dried and annealed at 100 °C for 20 hours prior to any measurement.

Instrumentation. *Size-exclusion chromatography (SEC).* Molar masses and polydispersity index were obtained by SEC using an Agilent 1260 Infinity HPLC system (equipped with pump, degasser, autosampler, and instant pilot controller); four Phenomenex Phenogel columns in series; a Wyatt TREOS ambient 3-angle light

scattering detector; and a Wyatt Optilab rEX differential refractive index detector. Ethyl acetate was used as the mobile phase at a flow rate of 1 ml/min.

Nuclear magnetic resonance (NMR). ^{1}H, ^{13}C, and ^{19}F NMR spectra were recorded on Varian Unity 500 wide bore multinuclear spectrometer with $CDCl_3$ as a solvent at room temperature.

Linear viscoelastic (LVE) measurement. Mechanical measurements of the bottlebrush polymers and macromonomer were performed on a Hybrid Rheometer 2 (TA Instruments) with 3 mm parallel plates. Small amplitude oscillatory shear was applied to the samples to evaluate their linear viscoelastic properties. The temperature was controlled by an Environmental Test Chamber with nitrogen as the gas source. The linear viscoelastic spectra were constructed based on the Time-Temperature Superposition Principle.

Transmission electron microscopy (TEM). These experiments were conducted on Zeiss LIBRA 120 operated at 120 kV acceleration voltages. A droplet of sample solution (4 μL, 1 mg/mL polymer concentration in EtOAc) was casted on copper grids (300 mesh, carbon film supported) and dried under ambient condition before TEM imaging. The TEM grids were then stained by OsO_4 vapor for two hours before taking TEM imaging.

Dynamic light scattering measurement (DLS). Dynamic light scattering measurements were carried out on a Compact Goniometer System (ALV) with four optical fiber based detection units with APD detectors, in the angular range 20–152°. The light source was a He-Ne laser of 632.8 nm with a power output of 22 mW. The normalized intensity autocorrelation function was computed by an ALV-7004 Multiple Tau Digital Correlator.

Atomic force microscopy (AFM). Images were collected on a Nanoscope IIIa Microscope with a multimode controller (Veeco Instruments) at room temperature by tapping mode with an antimony-doped Si tip (radius < 10 nm) at a line scanning frequency of 1 Hz. All

polymer thin films were store in vacuum oven at 100 °C for 20 h and slowly cooled to room temperature prior to the AFM measurements.

Contact angle measurement. Experiments were performed on a KRUSS DSA30 drop shape analysis system at ambient conditions. Water droplet (10 μL) was dropped through a syringe and equilibrated on the polymer coated silicon wafer for 30s prior to measurement. About five different spots on silicon wafer were tested, and recorded values are based on the average of five measurements.

Acknowledgements

This research was conducted at the Center for Nanophase Materials Sciences (CNMS) of Oak Ridge National Lab (ORNL), which is a DOE Office of Science User Facility. The authors would like to thank Drs. B. G. Sumpter, J.-M. Carrillo, M. Zhou, P. Bonnesen, and B. Lokitz for helpful discussions.

References

1 R. V. Iozzo, editor. *Proteoglycans: structure, biology, and molecular interactions*, Marcel Dekker: New York, 2000.

2 A. Varki, R. Cummings, J. Esko, H. Freeze, G. Hart, J. Marth, editors, *Essentials of glycobiology*, Cold Spring Harbor, NY: Cold Spring Harbor Laboratory Press, 1999.

3 S. S. Sheiko, B. S. Sumerlin, K. Matyjaszewski, *Prog. Polym. Sci.*, 2008, **33**, 759–785.

4 J. A. Johnson, Y. Y. Lu, A. O. Burts, Y. Xia, A. C. Durrell, D. A. Tirrell, R. H. Grubbs, *Macromolecules*, 2010, **43**, 10326–10335.

5 Z. Li, J. Ma, C. Cheng, K. Zhang, K. L. Wooley, *Macromolecules*, 2010, **43**, 1182–1184.

6 X. Li, S. L. Prukop, S. L. Biswal, R. Verduzco, *Macromolecules*, 2012, **45**, 7118–7127.

7 S. Peng, B. Bhushan, *RSC Advances*, 2012, **2**, 8557–8578.

8 B. R. Sveinbjörnsson, R. A. Weitekamp, G. M. Miyake, Y. Xia, H. A. Atwater, R. H. Grubbs, *PNAS*, 2012, **109**, 14332–14336.

9 Y. Xia, B. D. Olsen, J. A. Kornfield, R. H. Grubbs, *J. Am. Chem. Soc*., 2009, **131**, 18525–18532.

10 J. Scheirs, *Modern Fluoropolymers*, Wiley: New York, 1997.

11 L. Wang, B. C. Benicewicz, *ACS Macro Lett.*, 2013, **2**, 173–176.

12 N. M. L. Hansen, K. Jankova, S. Hvilsted, *Eur. Polym. J.*, 2007, **43**, 255–293.

13 A. M. Granville, S. G. Boyes, B. Akgun, M. D. Foster, W. J. Brittain, *Macromolecules*, 2005, **38**, 3263–3270.

14 M. Morita, H. Ogisu, M. Kubo, *J. Appl. Polym. Sci.*, 199**9**, **73**, 1741–1749.

15 G. Hougham, K. Johns, P. E. Cassidy, *Fluoropolymers: Synthesis and Properties*, Plenum: New York, 1999.

16 W. Yao, Y. Li, X. Huang, *Polymer*, 2014, **55**, 6197–6211.

17 A. Hirao, K. Sugiyama, H. Yokoyama, *Prog. Polym. Sci*., 2007, **32**, 1393–1438.

18 A. Tuteja, W. Choi, M. L. Ma, J. M. Mabry, S. A. Mazzella, G. C. Rutledge, G. H. McKinley, R. E. Cohen, *Science*, 2007, **318**, 1618–1622.

19 S. A. Brewer, C. R. Willis, *Appl. Surf. Sci*., 2008, **254**, 6450–6454.

20 G. He, G. Zhang, J. Hu, J. Sun, S. Hu, Y. Li, F. Liu, D. Xiao, H. Zou, G. Liu, *J. Fluorine Chem.*, 2011, **132**, 562–572.

21 T. Narita, T. Hagiwara, H, Hamana, *Macromol. Rapid Commun*., 1985, **6**, 175–178.

22 M. Semsarilar, V. Ladmiral, A. Blanazs, S. P. Armes, *Polym. Chem*., 2014, **5**, 3466–3475.

23 S. J. Dalsin, M. A. Hillmyer, F. S. Bates, *ACS Macro Lett*., 2014, **3**, 423–427.

24 K. L. Beers, S. G., Gaynor, K. Matyjaszewski, *Macromolecules*, 1998, **31**, 9413–9415.

25 Y. Schneider, J. D. Azoulay, R. Coffin, G. C. Bazan, *J. Am. Chem. Soc*., 2008, **130**, 10464–10465.

26 Y. Inoue, T. Matsugi, N. Kashiwa, K. Matyjaszewski, *Macromolecules*, 2004, **37**, 3651–3658.

27 K. Yamada, M. Miyazaki, K. Ohno, T. Fukuda, M. Minoda, *Macromolecules*, 1999, **32**, 290–293.

28 K. D. Dorkenoo, P. H. Peromm, M. E. Rezac, *J. Polym. Sci., Part B: Polym. Phys*., 1998, **36**, 797–803.

29 M. Zhang, A. H. E. Muller, *J. Polym. Sci., Part A: Polym. Chem*., 2005, **43**, 3461–3481.

30 Y. Tsukahara, K. Tsutsumi, Y. Okamoto, *Makromol. Chem. Rapid Commun*., 1992, **13**, 409–413.

31 Y. Tsukahara, S. I. Namba, J. Iwasa, Y. Nakano, K. Kaeriyama, M. Takahashi, *Macromolecules*, 2001, **34**, 2624–2629.

32 M. Hu, Y. Xia, G. B. McKenna, J. A. Kornfield, R. H. Grubbs, *Macromolecules*, 2011, **44**, 6935–6943.

33 C. R. Lopez-Barron, P. Brant, A. P. R. Eberle, D. J. Crowther, *J. Rheol.*, 2015, **59**, 865–883.

34 H. P. Hsu, W. Paul, S. Rathgeber, K. Binder, *Macromolecules*, 2010, **43**, 1592–1601.

35 S. L. Pesek, X. Li, B. Hammouda, K. Hong, R. Verduzco, *Macromolecules*, 2013, **46**, 6998–7005.

36 S. –K. Ahn, J. Y. Carrillo, Y. Han, T. –H. Kim, D. Uhrig, D. L. Pickel, K. Hong, S. M. Kilbey II, B. G. Sumpter, G. S. Smith, C. Do, *ACS Macro Lett.*, 2014, **3**, 862–866.

37 Y. Ma, X. Cao, X. Feng, Y. Ma, H. Zou, *Polymer*, 2007, **48**, 7455–7460.

38 J. A. Orlicki, N. O. L. Viernes, J. S. Moore, I. Sendijarevic, A. J. Hugh, *Langmuir*, 2002, **18**, 9990–9995.

39 M. Motornov, R. Sheparovych, E. Katz, S. Minko. *ACS Nano*., 2008, **2**, 41–52.

40 P. Roach, N. J. Shirtcliffe, M. I. Newton, *Soft Matter*., 2008, **4**, 224–240.

41 J. P. Youngblood, T. J. McCarthy, *Macromolecules*, 1999, **32**, 6800–6806.

42 A. Marmur, *Langmuir*, 2004, **20**, 3517–3519.